Int J Adv Manuf Technol
DOI 10.1007/s00170-012-3902-0

ORIGINAL ARTICLE

Development of a real-time laser-based machine vision system to monitor and control welding processes

Wei Huang · Radovan Kovacevic

Received: 8 April 2010 / Accepted: 5 January 2012

Abstract In this study, a laser-based machine vision system is developed and implemented to monitor and control welding processes. The system consists of three main modules: a laser-based vision sensor module, an image processing module, and a multi-axis motion control module. The laser-based vision sensor is designed and fabricated based on the principle of laser triangulation. By developing and implementing a new image processing algorithm on the platform of LabVIEW, the image processing module is capable of processing the images captured by the vision sensor, identifying the different types of weld joints, and detecting the feature points. Based on the detected feature points, the position information and geometrical features of the weld joint such as its depth, width, plates mismatch, and cross-sectional area can be obtained and monitored in real time. Meanwhile, by feeding these data into the multi-axis motion control module, a non-contact seam tracking is achieved by adaptively adjusting the position of the welding torch with respect to the depth and width variations of the weld joint. A 3D profile of the weld joint is also obtained in real time for the purposes of in-process weld joint monitoring and post-weld quality inspection. The results indicate that the developed laser-based machine vision system can be well suited for the measurement of weld joint geometrical features, seam tracking, and 3D profiling.

W. Huang · R. Kovacevic (✉)
Research Center for Advanced Manufacturing,
Southern Methodist University, RCAM-SMU,
3101 Dyer Street,
Dallas, TX 75205, USA
e-mail: kovacevi@engr.smu.edu

W. Huang
e-mail: huangw@smu.edu

Keywords Welding · Laser triangulation · Machine vision · Seam tracking · Feature extraction · Quality inspection

1 Introduction

In recent years, laser-based machine vision systems have been widely studied and developed for different manufacturing processes. The capabilities of the laser-based machine vision system to automate the manufacturing processes and greatly enhance the quality as well as the productivity attract much interest both from academia and industry. The metal industry that is using the welding processes to join two or more components made of ferrous and non-ferrous metals is also under great demand to improve the quality and productivity of the welding processes. As one of the key issues in the welding process, seam tracking is critical to the weld quality and productivity. First, seam tracking meets the need to fully automate the welding process. Nowadays, most of the welding robots that operate in industry are working in the teaching-and-playback mode, in which the position and motion path of the welding torch are predefined and taught point by point. Compared to automatic seam tracking, this teaching-and-playback mode is time-consuming, cost-inefficient, and not adaptive. Second, during the preparation phase of welding, modern techniques such as laser and plasma are commonly used to cut the profile of the joint groove. However, there are always inevitable cutting variations that need to be compensated by seam tracking to adaptively adjust the position of the welding torch to track the optimal welding path. Another reason for the requirement of seam tracking is to compensate for the weld deformation induced due to the thermal distortion and gravity distortion [1]. Besides seam tracking, in order to improve the weld quality, the varying geometrical features of the

Published online: 05 February 2012

weld joint also need to be monitored. Accordingly, the welding parameters need to be adaptively adjusted. In order to respond to these increasing requirements for improving weld quality and productivity, the welding industry is looking for new solutions by using advanced sensors and control devices. As a non-contact sensing technology, a laser-based machine vision system is widely studied and developed. Based on the principle of laser triangulation, the laser-based machine vision system was first developed to measure distance in a one-dimensional space [2]. As shown in Fig. 1, the sensor usually consists of a laser generator, an image receiver, and a focus lens. A high-quality laser beam is generated by a low-power diode laser, and the laser beam is projected onto the surface of the target. The laser light is then scattered by the surface of the target and reflected back into different directions. As an image receiver, a complementary metal oxide semiconductor (CMOS), or charge-coupled device camera is used to collect the reflected laser light. Therefore, the laser spot on the surface of the target will be imaged back on the image receiver at a certain position. In front of the image receiver, a focus lens is arranged at a specific distance and angle with respect to the image receiver to keep the images of the laser spot reflected from the target at different distances always focused on the image receiver. The distance between the laser-based vision sensor and the target can be precisely determined based on the mathematical relationship derived from geometrical optics. The accuracy of the measurement can be very high and configurable if the image receiver has a high resolution and the sensor itself is precisely designed based on geometrical optics [3].

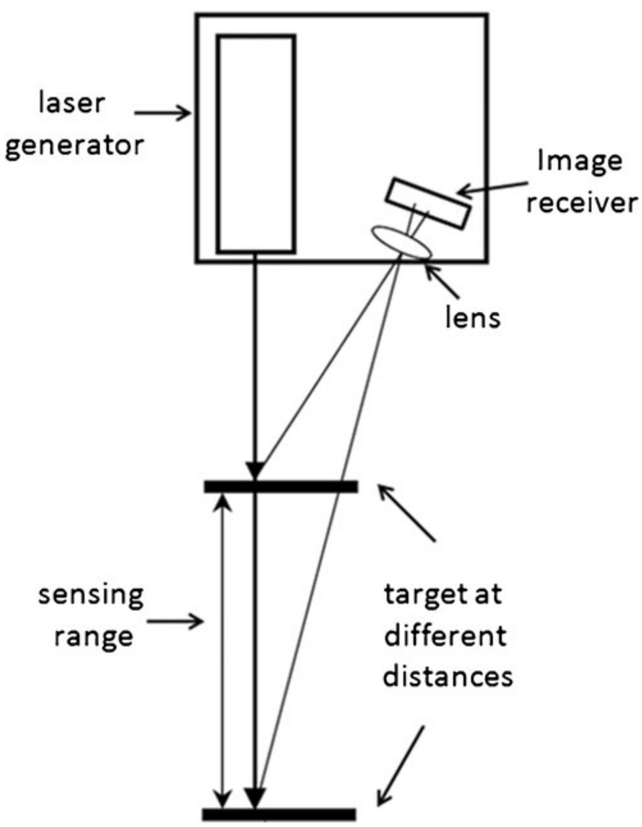

Fig. 1 Principle of laser triangulation. **a** Schematic of system setup [16], **b** photo of system setup

By extending the design principle of the laser-based vision sensor from a one-dimensional space to two-dimensional space, a structured-light laser stripe, instead of a laser beam, is projected onto the surface of the target. Therefore, the image of the projected laser stripe that follows the profile of the target can be acquired and processed to obtain the position information and geometrical features of the target. In the welding industry, the obtained position information of the weld joint is used to guide the welding torch to follow the optimal welding path so that the width and depth variations of the weld joint can be compensated during the welding process [4–6]. Meanwhile, the obtained geometrical features of the weld joint such as its width, depth, plates mismatch, and cross-sectional area can be used as the feedback to adaptively control the welding parameters and improve the weld quality as well as the productivity [7–9]. In addition to seam tracking and adaptive control, the laser-based machine vision system can also be used as a measurement tool [10, 11] and a 3D profiler [12, 13] for the purpose of in-process weld joint monitoring and post-weld quality inspection. Although the laser-based machine vision system has many advantages over traditional mechanical sensors, there are still some challenges. The most important issue related to laser-based machine vision system is the efficiency of the image processing algorithm. This issue is always critical because this algorithm is the main factor that limits the performance of the laser-based machine vision system. For its application in the welding process, the image processing algorithm should be able to obtain useful positioning information as well as the geometrical features of the weld joint. To obtain this information, the feature points of the weld joint such as the corner points of a groove need to be extracted precisely and efficiently. Current algorithms for detecting the feature points of the weld joint are mainly pattern recognition, Hough Transform, and line fitting. Pattern recognition uses a predefined template to match the geometrical features of the weld joint so as to extract the feature points of the weld joint. The involvement of convolution operation by using pattern recognition dramatically increases the computation load. On the other hand, both Hough Transform and line fitting for corner points detection are two-step processes. They first need to identify the main lines of the weld joint profile and then calculate the intersection points of these lines as the feature points of the weld joint. These three algorithms for detecting the feature points of the weld joint are computationally intensive and time-consuming, which greatly limits the performance of the system when high processing speed is needed. In order to improve the efficiency, reliability, and precision of the laser-based machine vision system, different patterns of laser, instead of a single structured-light laser strip, are used. Xu et al. [14] used a circular-patterned laser for seam tracking during robotic arc welding while Sung et al. [15] increased the number of laser stripes from one to five to improve the system efficiency. The proposed method only processes 20 images per second yet increases the system complexity. Besides the challenges related to the image processing algorithms, there are some problems related to the system hardware. From the perspective of the practical deployment of the laser-based machine vision system, the current commercially available cameras being used as the image receivers do not have a high frame rate that can satisfy the demand for high-speed welding even if the image processing algorithm can process the images efficiently. Additionally, the cable length between the camera and the image processing unit is greatly limited by the inherent property of the camera. This is a big disadvantage for the heavy metal industry that is dealing with the welding of large structures such as wind turbine towers, large heat exchangers and ships because a long cable between the sensor and the processing and control units is needed in these welding applications. In addition, the current laser-machine vision systems are mostly developed based on proprietary software and hardware, which are not flexible and are difficult to customize for different applications.

In order to tackle the abovementioned challenges, a real-time laser-based machine vision system is developed in this study. A laser-based vision sensor is designed and fabricated based on the principle of laser triangulation. A Gigabit Ethernet (GigE) camera, which has a high frame rate and can transfer image data at a maximum distance of 100 m, is adopted as the image receiver. A highly efficient yet easy-to-implement image processing algorithm is proposed and realized to process the stream of images acquired by the GigE camera, and extract the weld joint profile as well as the feature points for different types of weld joints. As a standard yet flexible off-the-shelf development platform, LabVIEW is used to develop the image processing module and the multi-axis motion control module in this study.

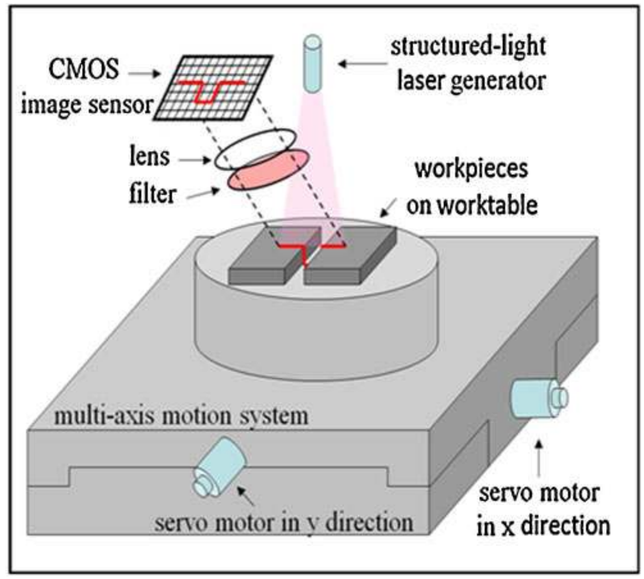

(a) Schematic of system setup [16]

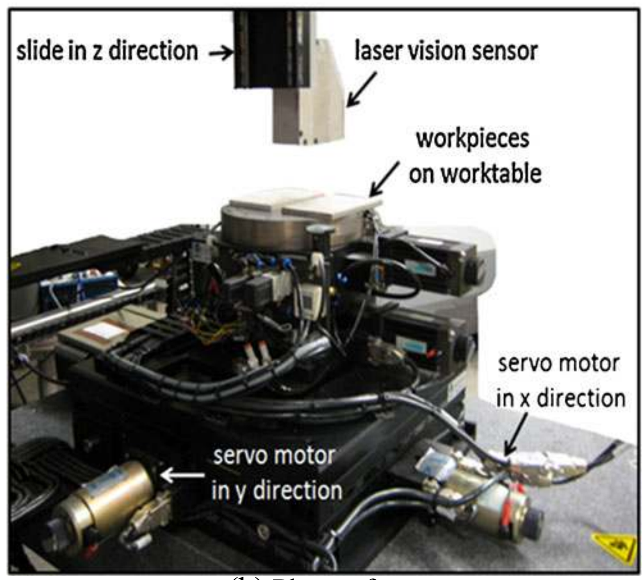

(b) Photo of system setup

Fig. 2 Experimental setup of the laser-based machine vision system. **a** Algorithm for laser stripe detection, **b** algorithm for corner point detection

2 Laser-based vision sensor design and system setup

As shown in Fig. 2, the laser-based machine vision system consists of three major modules: a laser-based vision sensor module, an image processing module, and a multi-axis motion control module. The laser-based vision sensor module incorporates a structured-light laser generator, a GigE camera, a lens, and an optical filter as shown in Fig. 2a. The structured-light laser generator perpendicularly projects a laser stripe with a wavelength of 657.9 nm onto the target workpieces placed on the worktable. In order to acquire the image of the reflected laser stripe that follows the profile of the target workpieces, a GigE camera with an embedded CMOS image sensor is arranged at a designed angle and distance with respect to the perpendicular reference plane of the projected laser stripe. The CMOS image sensor is a monochromatic sensor chip with a 659×494 array of 8-bit pixels. It can be used to acquire grayscale image with a light intensity ranging from 0 to 255, while 0 represents the lowest light intensity, and 255 represents the highest light intensity. The frame rate of the selected GigE camera is up to 200 frames per second, and the cable length is up to 100 m. In front of the camera, a lens is also precisely arranged in a designed distance and angle with respect to the image sensor chip in order to focus the reflected images of the laser stripe from different distances. In addition, a narrow-band optical filter centered at 658 nm is also placed in front of the focus lens. This optical filter is necessary to block out extraneous light generated during the welding process. Therefore, only the image of the reflected laser stripe in the wavelength of 657.9 nm can be obtained by the image sensor while the disturbance and noise from light in other wavelengths can be filtered out. By precisely designing the distance and angle between the image sensor chip and the focus lens, the position information as well as the geometrical features of the target workpieces can be calculated by the mathematical relationship derived from geometrical optics.

As shown in Fig. 2b, the designed and fabricated laser-based vision sensor module is placed in aluminum housing. The sensor is attached to a vertically movable slide above the worktable of the multiple-axis motion system. In order to achieve motion control for real-time seam tracking, a multi-axis motion system is involved to achieve movement in 3D space. The motion system has three servo motors while the two servo motors in the *x*- and *y*-directions are used to control the movements of the worktable horizontally. The third servo motor of the slide in the *z*-direction is used to control the movement of the attached laser-based vision sensor vertically. In this study, the two servo motors in the *x*- and *z*-directions will be simultaneously controlled by two analog voltage outputs from the image processing module to achieve seam tracking that compensates for the width and depth variations of the workpieces in these two directions. As mentioned above, the image processing module is critical to the performance of the whole vision system. The images acquired by the fabricated laser vision sensor are transferred to a computer through an Ethernet cable for further image processing where a control decision would be made to achieve seam tracking or adaptive control of the

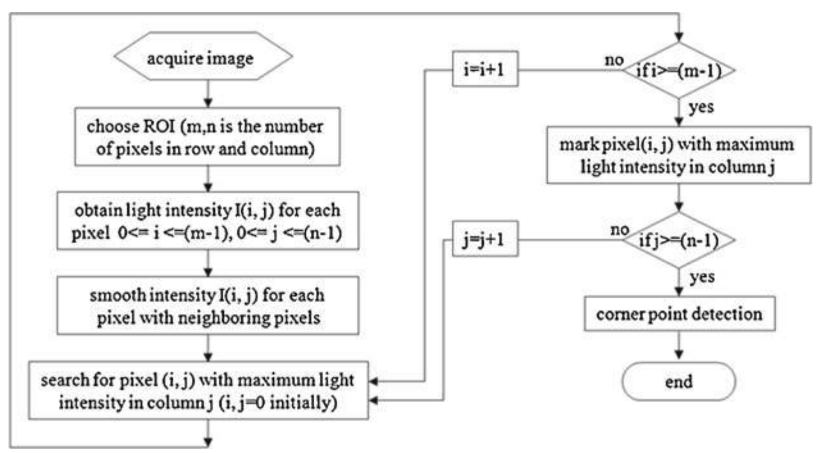

(a) algorithm for laser stripe detection

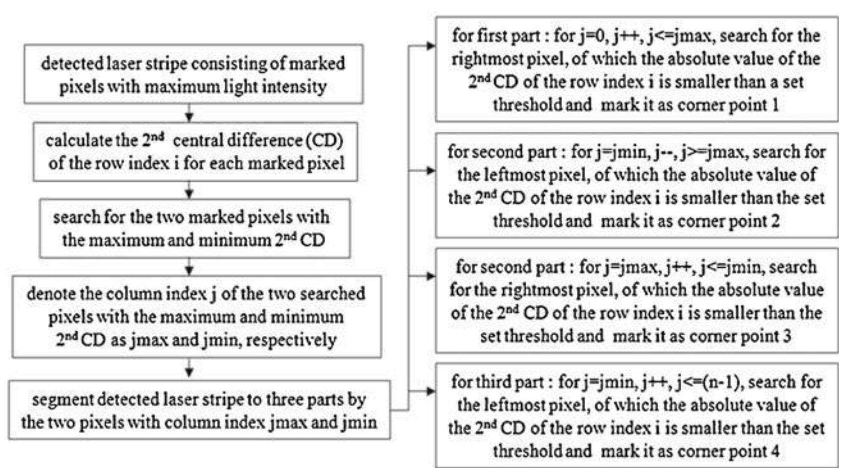

(b) algorithm for corner point detection

Fig. 3 Flowchart of the proposed image processing algorithm welding parameters based on the obtained position information and geometrical features of the weld joint.

3 Development of image processing algorithm

In order to obtain the position information as well as the geometrical features of the weld joint, the feature points such as the corner points of the joint groove need to be extracted. Before extracting the corner points, the laser stripe that follows the profile of the weld joint needs to be distinguished first. The digital grayscale image acquired by the camera can be considered as a pixel array in a size of 659×494. Since not all the parts of the image are of interest, a region of interest (ROI) with m rows and n columns of pixels can be chosen before processing the image. Properly choosing the ROI can dramatically decrease the amount of data that needs to be processed, reduce the processing time, and enhance the processing efficiency. After the ROI is chosen, the light intensity I(i, j) for each pixel in the ROI could be obtained. For each pixel, there is a corresponding value of the light intensity ranging from 0 to 255. The lowest light intensity corresponds to 0 while the highest light intensity corresponds to 255. In order to smooth the image for further processing and remove the noises in high frequency, the light intensity I(i, j) at each pixel is averaged with neighboring pixels by a Gaussian filter with a kernel size of 7×7. By considering the acquired image consisting of m rows and n columns of pixels, the pixel with the maximum light intensity in each column of the pixel array should be the one on the intersection between the vertical column of pixels and the horizontal pixels that represent the laser stripe. By searching for the pixel with the maximum light intensity at each column of the pixel array, a collection of such pixels that represent the laser stripe following the profile of the weld joint could be obtained. As shown in Fig. 3a, the flowchart generally illustrates how to process the acquired grayscale image to extract the pixels of the laser stripe. Since the laser stripe projected on the target has a thickness, more than 1 pixel in each column has the maximum intensity. Therefore, the middle one of those pixels that has the maximum light intensity is searched as the desired pixel to be extracted. After searching for all the pixels in each column with the maximum light intensity, the laser stripe that follows the profile of the weld joint is distinguishable from the ROI. Therefore, the column and row indexes of each extracted pixel can be used to extract the feature points of different weld joints.

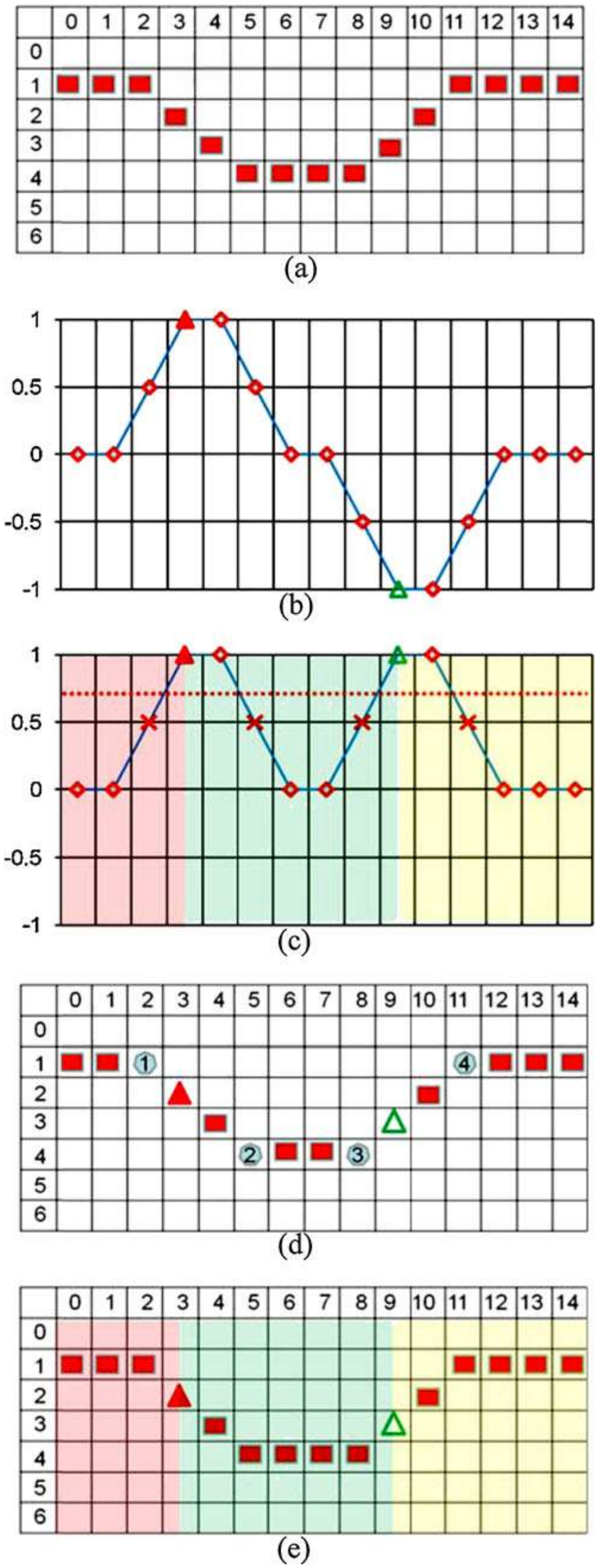

Fig. 4 Schematic illustration of proposed algorithm for corner point detection. **a** U-groove in the pixel space and coordinate space, **b** V-groove in the pixel space and coordinate space, **c** square-groove in the pixel space and coordinate space, **d** lap joint in the pixel space and coordinate space

For welding applications, the corner points at the edge of the weld groove are always considered as the feature points that need to be extracted to obtain the position information and geometrical features of the groove profile. In this study, in order to extract the corner points fast and efficiently, a new algorithm based on the second central difference (2nd CD) of the row index of each detected pixel on the laser stripe is proposed and implemented. As illustrated in Fig. 3b, the first step is to calculate the 2nd CD for the row index i of each detected pixel P (i, j) that represents the laser stripe. The 2nd CD of the row index of each pixel equal to half of the difference between the row indexes of the next pixel and the previous one. A schematic illustration of the proposed algorithm for corner point detection is shown in Fig. 4. A pixel array in a size of 7×15 as well as the detected pixels that represent the laser stripe is depicted in Fig. 4a. For the pixel P (1, 2), the 2nd CD can be calculated as half of the difference between the row indexes of pixel P (2, 3) and pixel P (1, 1), which is equal to 0.5×(2−1). Similar for pixel P (3, 9), the 2nd CD can be calculated as half of the difference between the row indexes of pixel P (2, 10) and pixel P (4, 8), which is equal to 0.5×(2−

Fig. 5 Image processing results

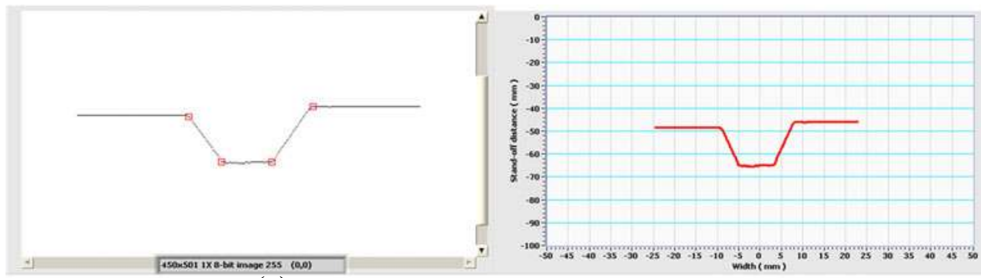

(a) U-groove in the pixel space and coordinate space

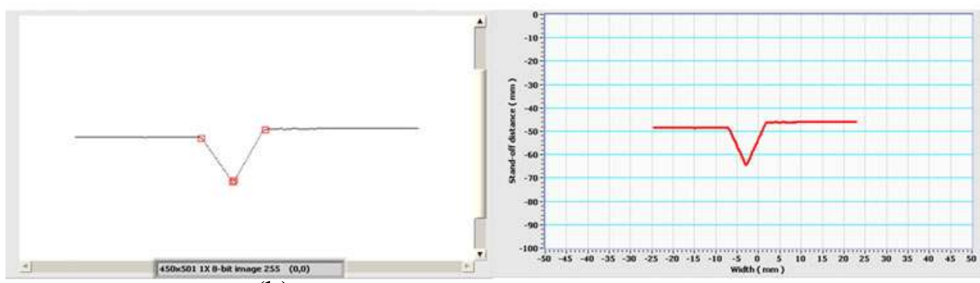

(b) V-groove in the pixel space and coordinate space

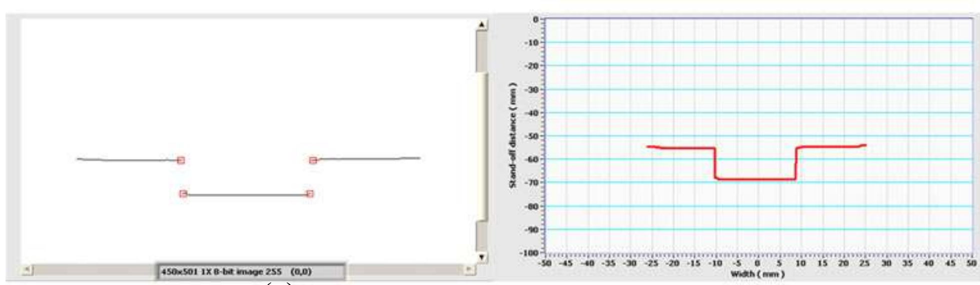

(c) square-groove in the pixel space and coordinate space

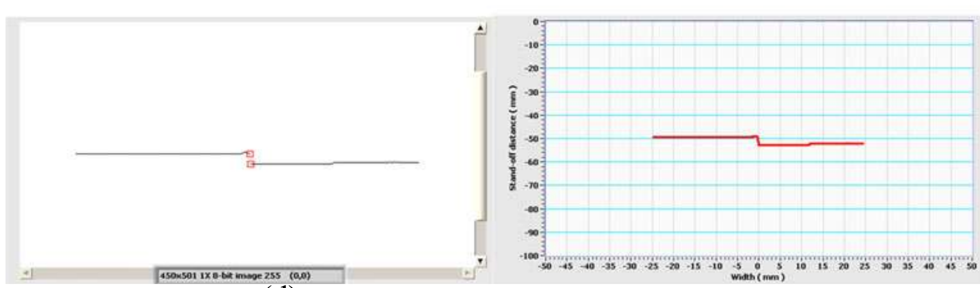

(d) lap joint in the pixel space and coordinate space

Fig. 6 Interface of laser-based machine vision system. **a** Coupon as a measurement target, **b** configuration of the measurement process

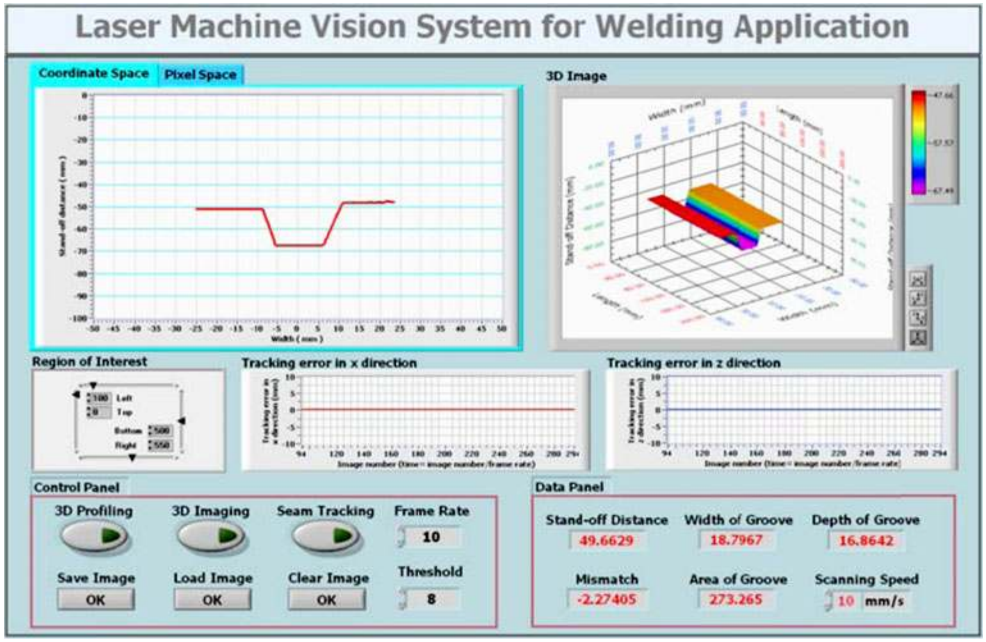

4). By calculating the 2nd CD for each pixel that is on the laser stripe, a result can be obtained in Fig. 4b. The second step is to search for the 2 pixels that have the maximum and minimum 2nd CD. As indicated by the solid and hollow triangle markers in Fig. 4b–c, the 2 pixels are searched as P (2, 3) and P (3, 9). The laser stripe is then segmented into three parts by the 2 pixels P (2, 3) and P (3, 9) as shown in Fig. 4c. By setting a threshold to the absolute value of the calculated 2nd CD of each pixel (the threshold is set to be 0.7 in the example and denoted by the dash line in Fig. 4d), the four corner points then can be detected based on the method detailed in Fig. 3b. For the instance of the first part of the laser stripe in Fig. 4d, the pixel P (1, 2) is the rightmost pixel whose 2nd CD is smaller than the set threshold. Therefore, this pixel can be marked as corner point 1 as depicted in the fifth graph in Fig. 4. The same method applies to the other two parts of the segmented laser stripe, and the other three corner points are also successfully detected and marked as shown in Fig. 4e.

As shown in Fig. 5, by implementing this proposed algorithm for corner point detection for four different types of weld joint configurations, such as U-groove, V-groove, square-groove, and lap joint, the profiles of the different weld joints in the coordinate space are successfully identified, and the position information of the weld joints with respect to the position of the laser vision sensor is obtained. Meanwhile, the corresponding corner points for each type of weld joints are also accurately detected in the pixel space while only minor revision of the proposed algorithm for corner point detection is needed for the different types of weld joint. The time consumed to process each frame of the image is around 3 ms, which means that more than 300 images can be processed to obtain the position information and geometrical features of the weld joints in 1 s. Compared to the most commonly used image processing algorithms for corner points detection such as pattern recognition, Hough Transform, and line fitting, which are computationally intensive, this new proposed image processing algorithm

Fig. 7 Setup for the measurement test and calibration. **a** Measurement of the standoff distance before calibration, **b** measurement of the width before calibration, **c** measurement of the thickness before calibration, **d** measurement of the width after calibration, **e** measurement of the thickness after calibration

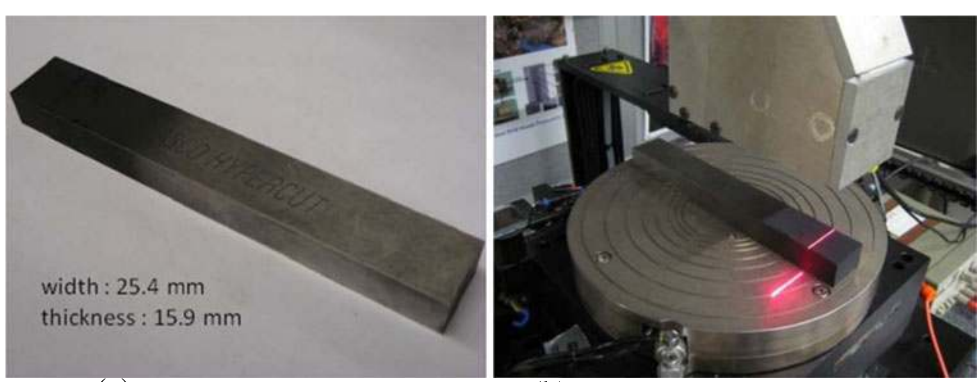

(a) coupon as a measurement target (b) configuration of the measurement process

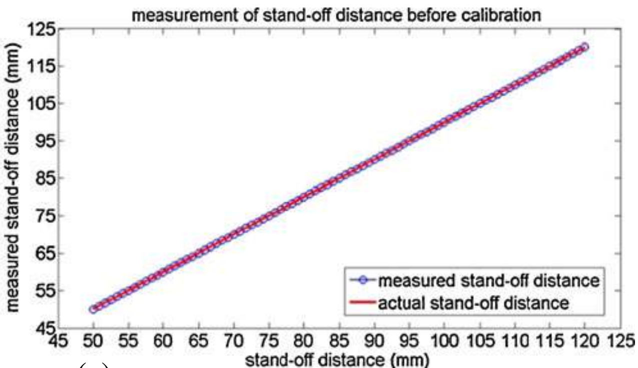

(a) measurement of the stand-off distance before calibration

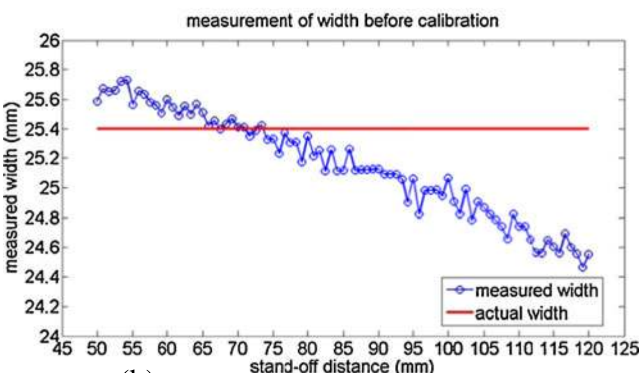

(b) measurement of the width before calibration

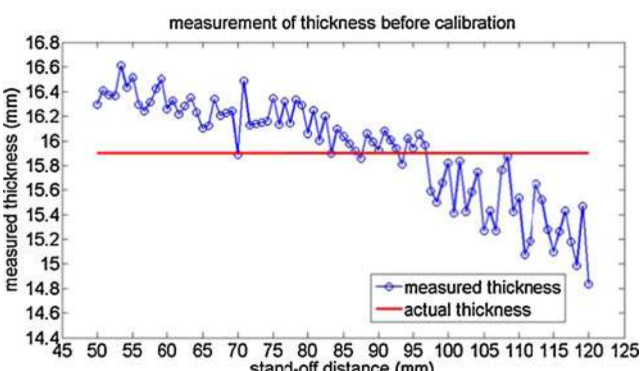

(c) measurement of the thickness before calibration

Fig. 8 Measurement results of the laser machine vision system. **a** Photo of the seam tracking configuration, **b** schematic of the top view of target workpiece, **c** schematic of the side view of target workpiece

based on the second central difference has a much higher processing efficiency and it is easy and straightforward to implement because it does not have to identify the main lines of the weld joint profile first like the other three commonly used algorithms. This preliminary image processing result offers the basis for other functions of the whole laser-based machine vision system such as the geometrical feature measurement, and seam tracking, as well as 3D profiling for the purpose of quality monitoring and inspection for different welding applications.

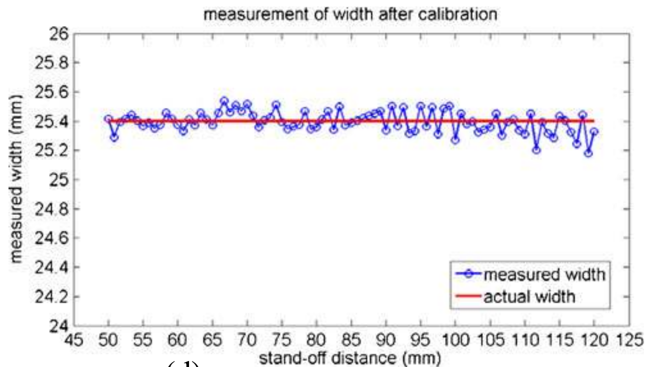

(d) measurement of the width after calibration

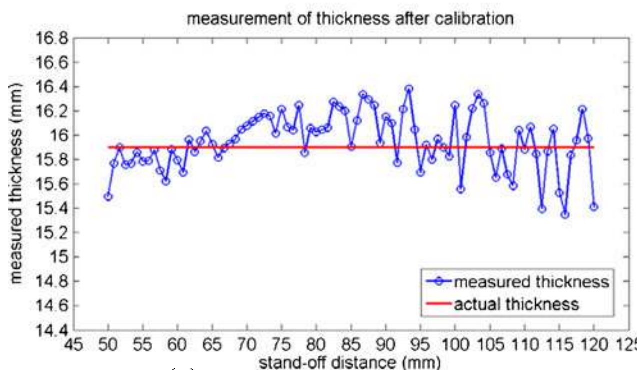

(e) measurement of the thickness after calibration

Fig. 8 (continued)

4 Real-time implementation of system in LabVIEW

After successfully proving the efficiency of the proposed image processing algorithm for laser stripe and corner points detection, the laser-based machine vision system is implemented in real time based on the platform of LabVIEW. As shown in Fig. 6, a LabVIEW-based program is developed to achieve multiple functions in real time such as image acquisition and processing, geometrical feature measurement, seam tracking, and 3D profiling. The human machine interface (HMI) of the laser-based machine vision system consists of several parts. At the top left corner of the HMI, the main window shows the detected laser stripe that follows the profile of the weld joint in the coordinate space with the calculated position and geometry information of the weld joint. With grids both in the *x*-direction (horizontal) and z-direction (vertical), the position information such as the vertical standoff distance between the bottom surface of the laser vision sensor and the top surface of the weld joint and the horizontal position of the weld joint with respect to the center of the laser vision sensor can be visualized. Meanwhile, the geometry features of the weld joint such as the width, depth, and plates mismatch as well as the cross-sectional area of the groove are also visually presented at the HMI. At the top right corner, the 3D profile of the workpieces is updated as the laser vision sensor scans the surface of the weld joint. The real-time generated 3D profile of the weld joint could be saved and reloaded when needed. The HMI also offers other features like choosing the ROI, the graphic indicator of tracking errors in the *x*- and *z*-directions, and the results of corner point detection in the pixel space as shown in Fig. 5.

4.1 Laser-based machine vision system as a measurement tool

The laser-based machine vision system is in its nature a measurement tool. The capability of the system to be used as a measurement tool represents the fundamental request to successfully fulfill the other functions of the system such as seam tracking with accurate motion control signals to compensate for the width and depth variations of the weld joint in XOZ plane and 3D profiling of the workpieces with precise dimensional and positional information for the purpose of in-process weld joint monitoring and post-weld quality inspection. In order to test and calibrate the laser-based machine vision system as a measurement tool, a coupon with a standard width of 25.4 mm and a thickness of 15.9 mm is used. As shown in Fig. 7a, the coupon is placed in such a way that it is perpendicular to the projected laser stripe so that the width of the coupon could be measured based on the two extracted corner points on the top surface of the coupon. The thickness of the coupon could also be measured by calculating the distance between the corner points on the top surface and bottom surface of the coupon. Also, the laser-machine vision system is also tested to measure the standoff distance between the bottom surface of the laser vision sensor and the top surface of the coupon. As shown in Fig. 7b, to test the stability and reliability of the laser-based machine vision system as a measurement tool at different standoff distances, the laser vision sensor is moved from a standoff distance of 50 mm to a standoff distance of 120 mm by controlling the slide motion in the *z*-direction to travel at a speed of 10 mm/s. The frame rate of the camera is set to be 12 frames per second. Therefore, 84 continuous measurements of the standoff distance, width, and thickness are carried out, and the measurement results are recorded and shown in Fig. 8a–c.

It can be observed from the measurement results before calibration that the measured standoff distance matches well with the actual standoff distances while the measured width and thickness of the coupon have some errors. From Fig. 8b–c, it can be observed that the maximum measurement errors of the width and thickness before calibration are 0.93 and 1.06 mm, respectively. By observing the measurement errors of the width and thickness, it also can be noted that the errors change with respect to the standoff distance and the trends of measured width and thickness of the coupon can be approximately depicted by a linear trendline with respect to the standoff distance. Therefore, in order to calibrate the laser-based machine vision system, two linear trendlines are calculated based on the minimum mean square error to depict the approximately linear relationship between the measured width and thickness with respect to the accurately measured standoff distance as shown in Eqs. 1 and 2, where S_m is the measured standoff distance, and W_{mt} and T_{mt} are the approximated width and thickness according to the calculated trendlines. As shown in Eqs. 3 and 4, the compensated values of width and thickness, W_c and T_c, to the meausred values are calculated by taking the

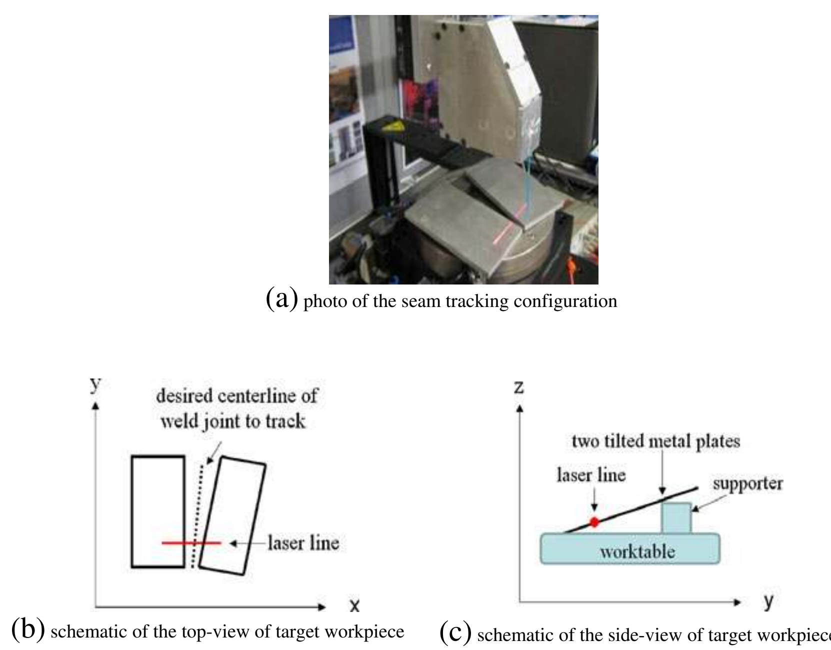

Fig. 9 Configuration of the workpieces for seam tracking

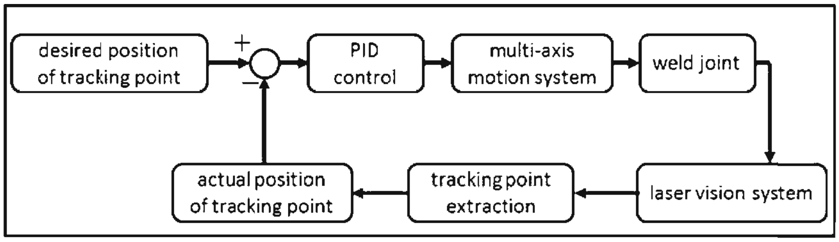

Fig. 10 Flowchart of the close-loop control for seam tracking. **a** Error in the *x*-direction without seam tracking, **b** error in the *z*-direction without seam tracking, **c** error in the *x*-direction with seam tracking, **c** error in the *z*-direction with seam tracking

difference between the actual width or thickness of the coupon and the approximated corresponding values. These two compensated values of the width and thickness are then added to the measured width W_m and thickness T_m and finally the calibrated measurements of width W and thickness T are obtained as shown in Eqs. 5 and 6.

$$W_{mt} = -0.0166 \times S_m + 26.57 \quad (1)$$

$$T_{mt} = -0.0175 \times S_m + 17.428 \quad (2)$$

$$W_c = 25.4 - (-0.0166 \times S_m + 26.57) = 0.0166 \times S_m - 1.17 \quad (3)$$

$$T_c = 15.9 - (-0.0175 \times S_m + 17.428) = 0.0175 \times S_m - 1.528 \quad (4)$$

$$W = W_m + W_c \quad (5)$$

$$T = T_m + T_c \quad (6)$$

As shown in Fig. 8d–e, the process of the continuous measurements of the width and thickness of the coupon is carried out again after calibration is done. The calibrated measurement of the width has a maximum error of 0.22 mm, and the calibrated measurement of the thickness has a maximum error of 0.55 mm, which is a dramatic improvement with respect to the measurement results before calibration. By observing the calibrated measurement results, it can be noted that the measurement errors of width and thickness are increased as the standoff distance is increased. This is related to the sensing range of this laser vision sensor that goes from a standoff distance of 11.25 mm to a standoff distance of 148.93 mm. When the standoff distance increases, the resolutions of the measurement in both the *x*- and *z*-directions decrease. When the standoff distance is at 11.25 mm, the lateral and vertical resolutions are 0.06 and 0.14 mm/pixel,

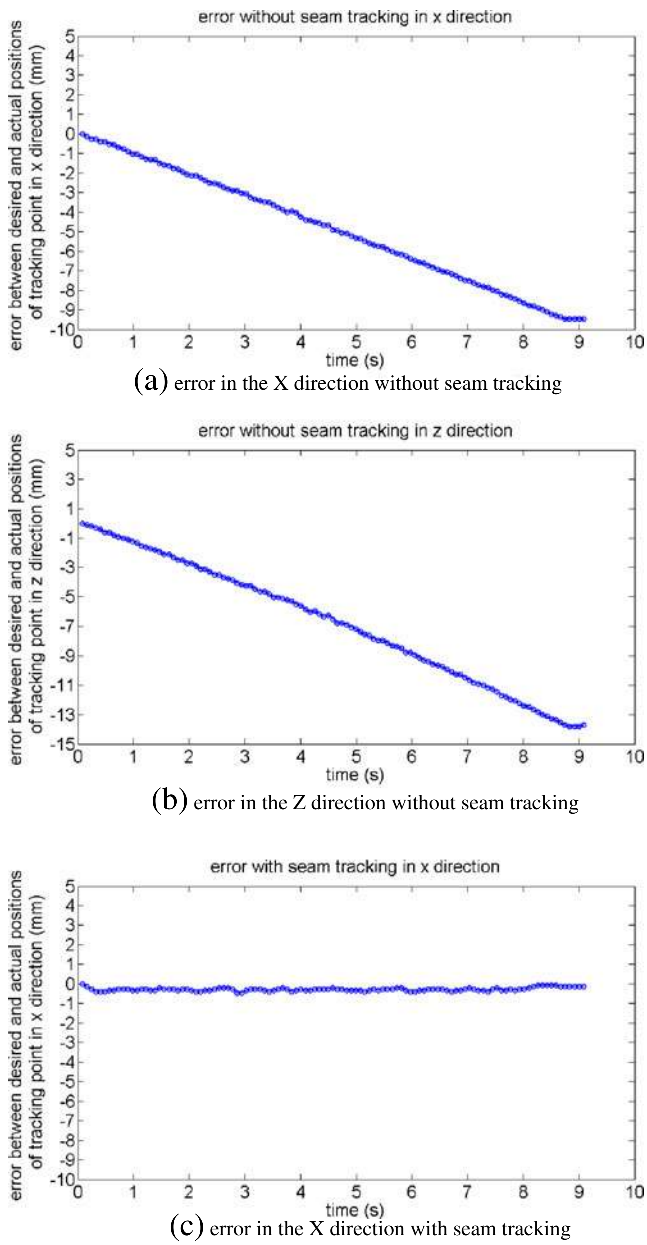

Fig. 11 Results of the laser machine vision system for seam tracking. **a** 3D view of the groove without seam tracking, **b** 3D view of the groove with seam tracking, **c** top view of the groove without seam tracking, **d** top view of the groove with seam tracking, **e** side view of the groove without seam tracking, **f** side view of the groove with seam tracking

Fig. 12 Scanning results of weld groove during the activated and deactivated seam tracking process. **a** Coupon as a post-weld inspection target, **b** configuration of the inspection process

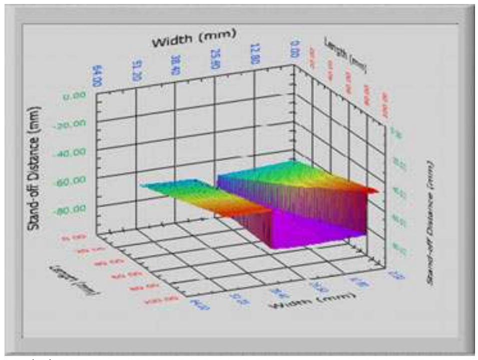

(a) 3D-view of the groove without seam tracking

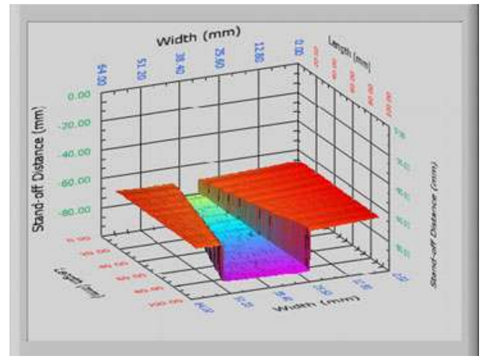

(b) 3D-view of the groove with seam tracking

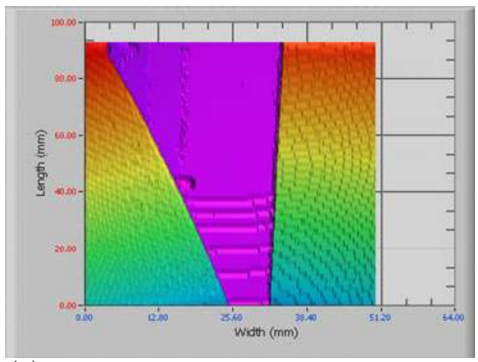

(c) top-view of the groove without seam tracking

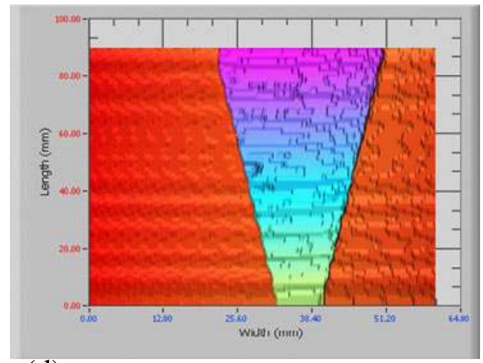

(d) top-view of the groove with seam tracking

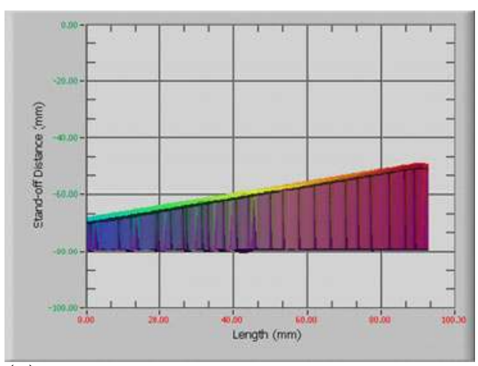

(e) side-view of the groove without seam tracking

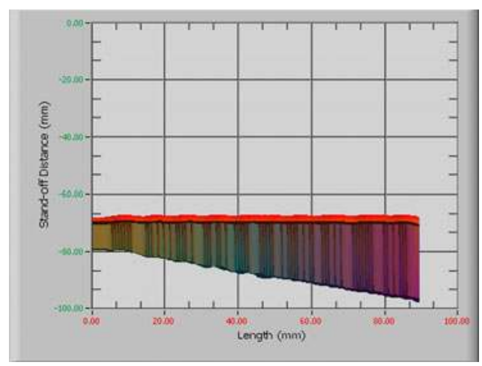

(f) side-view of the groove with seam tracking

respectively. And when the standoff distance is at 148.93 mm, the lateral and vertical resolutions are 0.24 and 1 mm/pixle, respectively. This explains why the measurement errors of width and thickness of the coupon increase when the standoff

Fig. 13 Setup for post-weld inspection. **a** 3D view of the scanned coupon, **b** top view of the scanned coupon, **c** side view of the scanned coupon

(a) coupon as a post-weld inspection target

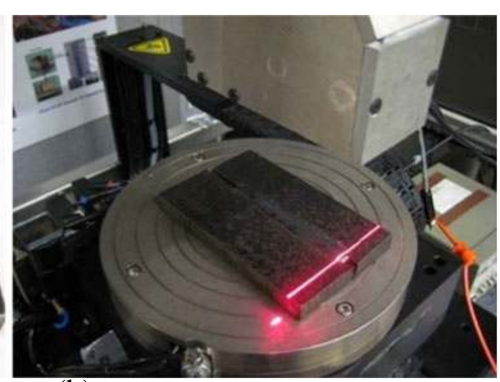

(b) configuration of the inspection process distance increases. Since the lateral resolution is always higher than the vertical resolution and it does not change as much as the vertical resolution does, the calibrated measurement of the width is more accurate than the calibrated measurement of the thickness. Therefore, in order to achieve a better performance of the sensor, it is preferable to keep the standoff distance between the laser vision sensor and the target in a proper range. By accurately measuring the positional and geometrical information of the weld joint, other functions such as seam tracking, 3D profiling as well as the adaptive control of welding parameters based on real-time monitoring of the weld joint geometry can be further achived.

4.2 Laser-based machine vision system for seam tracking

As shown in Fig. 9, in order to test the performance of system for seam tracking, two metal plates are arranged in a way that both the width and height of the groove change along the *y*-direction. The desired tracking point is the center of the two corner points on the top surface of the two metal plates, which is depicted by the dashed line as shown in Fig. 9b. Meanwhile, as shown in Fig. 9c, the system should also be able to follow the height change of the tracking point in the *z*-direction by adaptively controlling the slide vertically. In the *y*-direction, the worktable of the motion system is programmed to move at a constant speed of 10 mm/s with a travel distance of 90 mm. As the worktable moves along the *y*-direction, the position of the desired tracking point changes accordingly. To follow this change, the servo motors of the motion system both in the *x*- and *z*-directions must fast and adaptively move horizontally and vertically to compensate for the position error between the desired and actual position of the tracking point. Figure 10 shows the schematic of the close-loop PID control of the servo motors in the *x*- and *z*-directions by outputting two analog voltage signals from the image processing module. By applying this close-loop control, the seam tracking is successfully carried out. Figure 11a–b shows the errors between the desired and actual position of the tracking point in the *x*- and *z*-directions without seam tracking. The large errors are induced because the seam tracking is not activated to compensate for the position error along the *x*- and *z*-directions when the worktable constantly moves along the *y*-direction. By contrast, as shown in Fig. 11c–d, the tracking along the *x*- and *z*-directions is achieved with an accuracy of ±0.5 mm when seam tracking is activated.

Figure 12a–f shows the 3D profiles of the workpiece groove scanned by the developed laser-based machine vision system. Figure 12a, c, e shows scanned profiles of the groove when the seam tracking is not activated while Fig. 12b, d, f show the scanned profile while the seam tracking is activated. By comparing the two top views of the profile of the groove in Fig. 12c–d, it can be observed that when the seam tracking is activated, the profile of the groove from the top view is symmetrical, because the laser vision sensor has successfully tracked the center of the top two corner points of the groove. By comparing the two side views of the profile of the groove in Fig. 12e–f, it could also be noted that when the seam tracking is not activated, the position of the laser vision sensor does not follow the height change of the groove. Therefore, the profile of the groove in the side view exactly shows the height increase of the groove along the *y*-direction. Conversely, when the seam tracking is activated, the position of the laser vision sensor follows the height increase of the groove and compensates

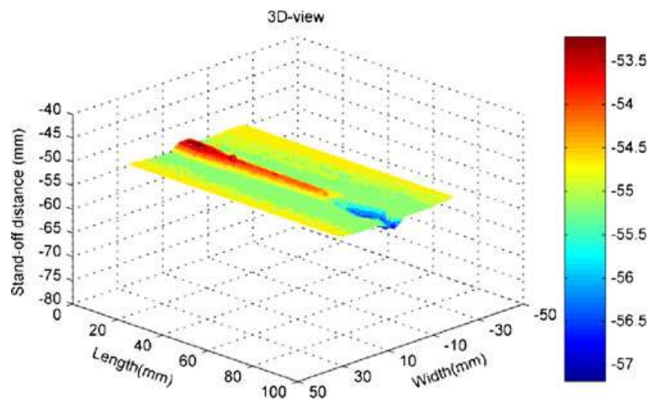

(a) 3D-view of the scanned coupon

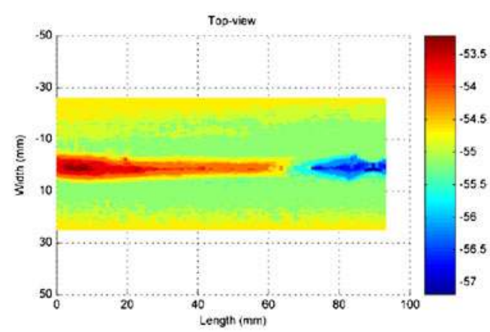

(b) top-view of the scanned coupon

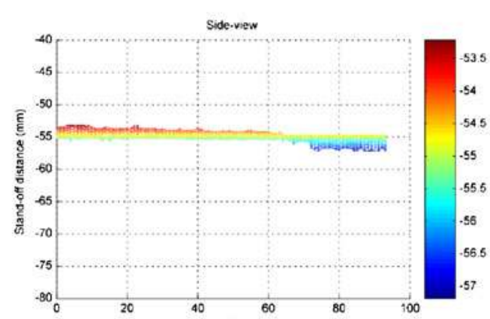

(c) side-view of the scanned coupon

Fig. 14 Results of post-weld inspection with the laser-based machine vision system for the change in the height. As a result, the profile of the tilted top surface of the two metal plates is flat as shown in Fig. 12f.

4.3 Laser-based machine vision system for 3D profiling

Besides the functions of geometry measurement and seam tracking, the laser-based machine vision system is also capable of in-process weld joint monitoring and post-weld quality inspection by scanning the 3D profile of the welds. As shown in Fig. 13, a weld bead obtained by a hybrid fiber laser and gas metal arc welding of thick plates is used as the coupon for system testing. The profile of the weld bead is uniform at the beginning while there is a crater at the end of the weld. In order to obtain the 3D profile of this weld bead with the developed laser-based machine vision system, the worktable moves along the *y*-direction so that the laser vision sensor can fully scan the full length of the weld bead at a constant speed. As shown in Fig. 14, the 3D profile of the scanned coupon is obtained, saved, and reloaded in Matlab. The 3D view and top view of the profile shown in Fig. 14a–b clearly indicates the presence of the crater at the end of the weld bead. The side view of the profile in Fig. 14c also shows the height change of the weld bead as well. Also, the different views of the profile of the scanned coupon accurately show the width, and height as well as the position and size of the crater, which is very useful for post-weld quality inspection.

5 Conclusions

In this paper, a real-time laser-based machine vision system is developed. A laser vision sensor is designed and fabricated based on the principle of laser triangulation. The application of the GigE camera involved in the design of the sensor overcomes the limits of the currently used cameras for a commercially available laser-based machine vision system. The developed laser-based machine vision system allows transferring the acquired images to an industrial computer at a high frame rate and a distance up to 100 m. By proposing and implementing a new image processing algorithm for the detection of the laser stripe and corner points based on the LabVIEW development platform, each image can be successfully processed in about 3 ms. This proposed image processing algorithm greatly increases the efficiency and simplifies the programming if there is a need to introduce a different configuration of the weld. As a measurement tool, the accuracy of the developed system is in an acceptable range (±0.55 mm). By simultaneous control of the two axes of the motion system, seam tracking of the weld groove is also achieved fast and accurately. Also, the 3D profiling of the weld in real time allows the laser-based machine vision system to be used as an in-process weld joint monitoring and post-weld quality inspection tool to detect and identify the visually recognized weld defects. The prototype of the developed laser-based machine vision system is designed with a very large field of view. However, this design with a large field of view also compromises the resolution of the laser vision sensor and the accuracy of the measurement and seam tracking. As mentioned above, the resolution of the laser-based machine vision system is reconfigurable by changing the optical design of the laser vision sensor. Therefore, for different welding applications, a different laser-based machine vision system can be correspondingly designed and implemented to meet specific requirements of the resolution and accuracy.

Acknowledgments This research was partly financially supported by the National Science Foundation under grant no. EEC-0541952. Thanks to Mr. Andrew Socha, research engineer of the Research Center for Advanced Manufacturing (RCAM) at SMU and Perry Leggett, a PhD candidate at RCAM, for their great assistance in this research.

References

1. Li Y, Xu D, Yan Z, Yan M (2006) Girth seam tracking system based on vision for pipe welding robot. Proceeding of 2006 International Conference on Robotic Welding, Intelligence and Automation, Shanghai, China, December 8–11, 2006
2. Mayer R (1999) Scientific Canadian: invention and innovation from Canada's National Research Council. Raincoast Books, Vancouver
3. Keferstein CP, Marxer M (1998) Testing bench for laser triangulation sensors. Sensor Review 18(3):183–187
4. Lee SK, Chang WS, Yoo WS, Na SJ (2000) A study on a vision sensor based laser welding system for bellows. J Manuf Syst 19 (4):249–255
5. Lee SK, Na SJ (2002) A study on automatic seam tracking in pulsed large edge welding by using a vision sensor without an auxiliary light source. J Manuf Syst 21(4):302–315
6. Luo H, Chen XQ (2005) Laser visual sensing for seam tracking in robotic arc welding of titanium alloys. Int J Adv Manuf Technol 26 (9–10):1012–1017
7. Moon HS, Beattie RJ (2002) Development of adaptive fill control for multitorch multipass submerged arc welding. Int J Adv Manuf Technol 19(12):867–872
8. Bae KY, Lee TH, Ahn KC (2002) An optical sensing system for seam tracking and weld pool control in gas metal arc welding of steel pipe. Journal of Material Processing Technology 120(1–3):458–465
9. Chen Z, Song Y, Zhang J, Zhang W, Jiang L, Xia X (2007) Laser vision sensing based on adaptive welding for aluminum alloy. Frontier of Mechanical Engineering in China 2(2):218–223
10. Peng Y, Kumehara H, Zhang W (2007) Measurement of drill point geometry by using laser sensor. Int J Mach Tool Manuf 47(3–4):682–688
11. Huang SJ, Lin YW (1996) A prototype system of three-dimensional non-contact measurement. Int J Adv Manuf Technol 11(5):336–342

12. Son S, Park H, Lee KH (2002) Automated laser scanning system for reverse engineering and inspection. Int J Mach Tool Manuf 42 (8):889–897
13. Sodhi MS, Tiliouine K (1996) Surface roughness monitoring using computer vision. Int J Mach Tool Manuf 36(7):817–828
14. Xu P, Xu G, Tang X, Yao S (2008) A visual seam tracking system for robotic arc welding. Int J Adv Manuf Technol 37(1–2):70–75
15. Sung K, Lee H, Choi YS, Rhee S (2009) Development of a multiline laser vision sensor for joint tracking in welding. Weld J 4:79–85
16. Noruk, J. & Boillot, J. P. (2006) Laser vision technology ensures six sigma-level quality is achieved in robotic welding. Canadian Welding Association Journal, Summer 2006, 8–14